

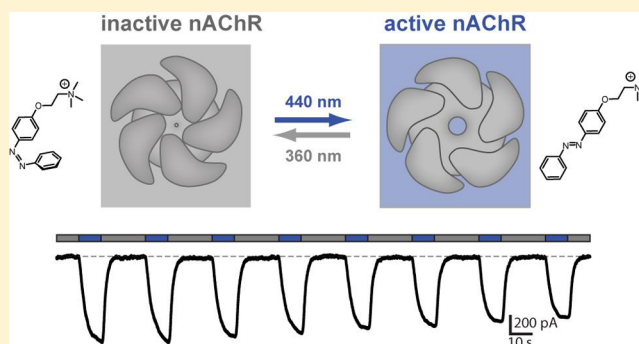
## AzoCholine Enables Optical Control of Alpha 7 Nicotinic Acetylcholine Receptors in Neural Networks

Arunas Damijonaitis,<sup>†</sup> Johannes Broichhagen,<sup>†</sup> Tatsuya Urushima,<sup>†</sup> Katharina Hüll,<sup>†</sup> Jatin Nagpal,<sup>‡</sup> Laura Laprell,<sup>†</sup> Matthias Schönberger,<sup>†</sup> David H. Woodmansee,<sup>†</sup> Amir Rafiq,<sup>§</sup> Martin P. Sumser,<sup>†</sup> Wolfgang Kummer,<sup>§</sup> Alexander Gottschalk,<sup>‡</sup> and Dirk Trauner<sup>\*,†</sup><sup>†</sup>Department of Chemistry and Pharmacology, Ludwig-Maximilians-Universität München, Center of Integrated Protein Science Munich, Munich D-81377, Germany<sup>‡</sup>Buchmann Institute for Molecular Life Sciences, Institute of Biochemistry, Johann Wolfgang Goethe-Universität, Frankfurt D-60438, Germany<sup>§</sup>Institute for Anatomy and Cell Biology, Justus-Liebig-Universität, German Center for Lung Research, Giessen D-35385, Germany

## Supporting Information

**ABSTRACT:** Nicotinic acetylcholine receptors (nAChRs) are essential for cellular communication in higher organisms. Even though a vast pharmacological toolset to study cholinergic systems has been developed, control of endogenous neuronal nAChRs with high spatiotemporal precision has been lacking. To address this issue, we have generated photoswitchable nAChR agonists and re-evaluated the known photochromic ligand, BisQ. Using electrophysiology, we found that one of our new compounds, AzoCholine, is an excellent photoswitchable agonist for neuronal  $\alpha 7$  nAChRs, whereas BisQ was confirmed to be an agonist for the muscle-type nAChR. AzoCholine could be used to modulate cholinergic activity in a brain slice and in dorsal root ganglion neurons. In addition, we demonstrate light-dependent perturbation of behavior in the nematode, *Caenorhabditis elegans*.

**KEYWORDS:** Photopharmacology, photochromic ligand, AzoCholine, BisQ, nicotinic acetylcholine receptor, cholinergic system



Acetylcholine (ACh) is a classic neurotransmitter that is critically involved in a variety of neural functions, such as movement, cognition, and memory.<sup>1,2</sup> After presynaptic release, it acts on muscarinic and nicotinic acetylcholine receptors (mAChRs and nAChRs, respectively). nAChRs are found at the neuromuscular end plate in the periphery and on a variety of cholinergic synapses in the central and the peripheral nervous system. To date, 12 neuronal and 5 neuromuscular nAChR subunits have been described in mammals, which assemble as homo- or heteropentamers. While the fetal neuromuscular nAChRs consist of  $\alpha 1$ -,  $\beta 1$ -,  $\delta$ -, and  $\gamma$ -subunits, the  $\gamma$ -subunit is exchanged for the  $\epsilon$ -subunit in adults (Figure 1a). Neuronal nAChRs can consist of  $\alpha$ ,  $\beta$  combinations (made up from  $\alpha 2$ – $\alpha 10$  and  $\beta 2$ – $\beta 4$ ) or as  $\alpha 7$ – $\alpha 9$  homopentamers.<sup>1,2</sup>

The combinatorial diversity and widespread occurrence of nAChRs require highly selective and precise tools for investigating cholinergic signaling. Therefore, sensitizing these receptors toward light could be advantageous (Figure 1c). In pioneering studies by Erlanger's group in the late 1960s, a photosensitive azobenzene-derived nAChR agonist, called BisQ (Figure 1d), was used to modulate the membrane potential of the electroplax organ of *Electrophorus electricus* in a light-dependent manner.<sup>3–5</sup> Following up on this, Lester charac-

terized BisQ and other photochromic compounds as photoisomerizable nicotinic agonists and muscarinic antagonists.<sup>6–8</sup> With the advent of modern photopharmacology,<sup>9,10</sup> which relies on molecular cloning and heterologous expression of transmembrane receptors as well as modern light delivery techniques (e.g., LEDs), it is possible to investigate individual receptors in more detail. This has been done, for instance, using the photoswitchable tethered ligand approach, which yielded the light-controlled nAChR (LinAChR). LinAChR consists of a nAChR agonist, an azobenzene photoswitch, and a maleimide that is covalently attached to engineered cysteines of  $\alpha 3\beta 4$  or  $\alpha 4\beta 2$  nAChR.<sup>11</sup>

Freely diffusible photochromic ligands (PCLs) combine the advantages of conventional pharmacology with the spatiotemporal precision of light. They have been used to optically control ion channels,<sup>12–17</sup> metabotropic receptors,<sup>18,19</sup> and enzymes.<sup>20</sup> Here, we revisit the classic PCL BisQ and describe the development of PCLs for neuronal nAChRs. One of these compounds, AzoCholine, could be used to control the activity

Received: January 20, 2015

Revised: March 3, 2015

Published: March 5, 2015

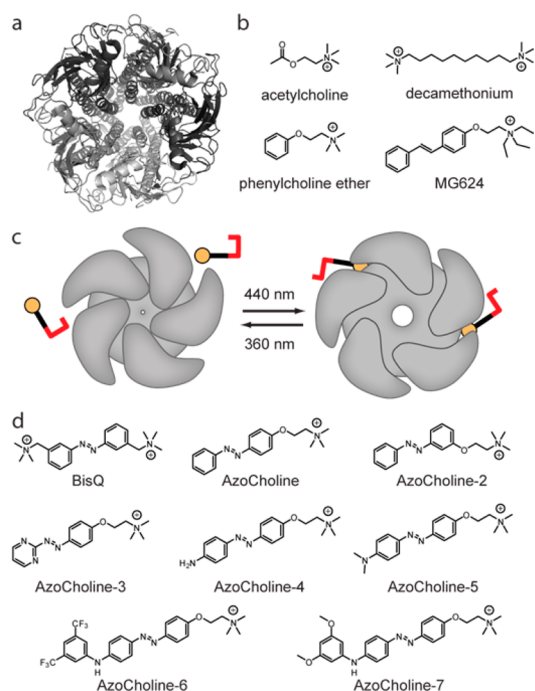


**Figure 1.** Structural model of a nAChR, chemical structures of nAChR ligands, and schematic function of PCLs. (a) Structural model derived from cryoelectron microscopy data of a neuromuscular nAChR (top-view) (PDB: 2bg9).<sup>21</sup> (b) Chemical structures of AChR ligands. (c) Schematic representation of the light-dependent activation of a nAChR with a PCL. (d) Chemical structures of azobenzene-containing PCLs designed to act on nAChRs.

of dorsal root ganglion (DRG) and hippocampal neurons as well as the behavior of the nematode, *Caenorhabditis elegans* (*C.elegans*), with light.

## RESULTS AND DISCUSSION

**Design and Synthesis of PCLs.** To develop a photoswitchable version of ACh that acts on neuronal nAChRs, we prepared a series of photoswitchable derivatives of the known agonist, phenylcholine ether (Figure 1b). These compounds, AzoCholine and its congeners AzoCholine 2–7 (Figure 1d), also bear resemblance to the  $\alpha 7$  nAChR antagonist MG624 (Figure 1b). The synthesis of AzoCholine is shown in Figure 2. Exposure of 4-hydroxy azobenzene (**1**) to 2-chloro-*N,N*-dimethylethylamine hydrochloride gave tertiary amine **2**. Quarternarization of the amine with methyl iodide then yielded AzoCholine (Figure 2a). Its structure in the solid state is shown

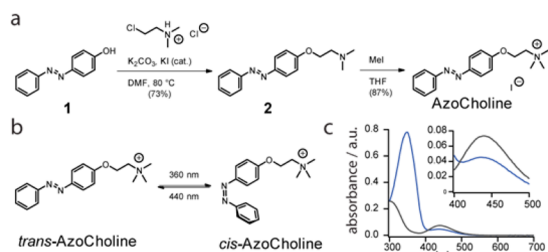


**Figure 2.** Synthesis and switching of AzoCholine. (a) Two-step synthesis. (b) *Cis/trans* isomerization. (c) UV/vis spectra of AzoCholine (50  $\mu$ M in DMSO at room temperature) irradiated with 360 nm (gray line) and 440 nm (blue line) light. The inset shows a magnification of the  $n-\pi^*$  band.

in the Supporting Information (Figure S1a). AzoCholine could be switched between its *cis* and *trans* state by irradiation with 360 and 440 nm light, respectively (Figure 2b). The UV/vis spectra of AzoCholine irradiated with these wavelengths are shown in Figure 2c. The synthesis of AzoCholines 2–7 is discussed in the Supporting Information (pages 6–15). While some of these compounds showed red-shifted absorption spectra and reversible switching (Figure S2), the simplest member of the series, AzoCholine, emerged as the most effective PCL. Therefore, our physiological studies focused on this compound and BisQ.

BisQ is derived from decamethonium (Figure 1b), as described by Erlanger.<sup>3–5</sup> We improved on the original synthesis and devised a four-step procedure, which relied on a Mills reaction to create the azobenzene moiety (see Supporting Information, pages 3–5).

**AzoCholine Is a Photoswitchable Agonist for the  $\alpha 7$  nAChR.** To characterize the action of our PCLs on a neuronal receptor, we heterologously expressed an  $\alpha 7$  nAChR/glycine receptor chimera in HEK293T cells.<sup>22</sup> This chimeric channel is a pharmacological model for the neuronal  $\alpha 7$  nAChR<sup>23</sup> with the advantage of high expression levels in HEK293T cells. Action spectra were recorded using patch-clamp electrophysiology to determine the optimal wavelengths for activation and inactivation of the receptors (Figure S3).

Interestingly, BisQ showed no notable activation of the chimeric  $\alpha 7$  nAChR at 50  $\mu$ M concentration (induced current:  $5.93 \pm 2.81$  pA, i.e.,  $1.15 \pm 0.64\%$  normalized to ACh) (Figures 3a and S4). By contrast, AzoCholine (50  $\mu$ M) proved to be a potent agonist in its *trans* state, inducing a current of  $691.81 \pm 278.65$  pA (Figure 3b). Normalized with respect to the natural ligand, ACh (50  $\mu$ M) (Figure 3c), illumination of AzoCholine with blue light evoked currents almost twice as large ( $223.66 \pm 30.06\%$ ) (Figure 3d). This process was reversible by alternating

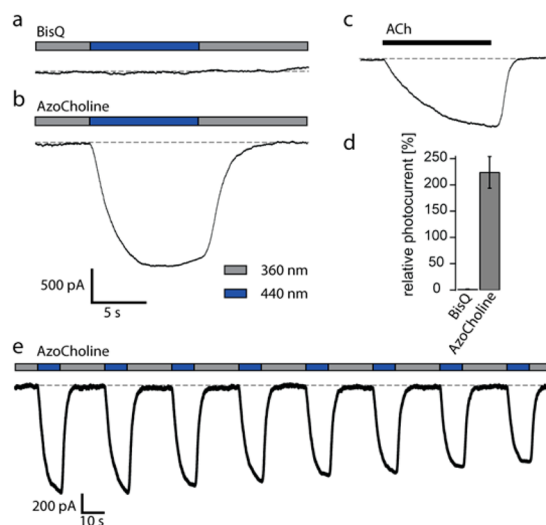


**Figure 3.** Light-dependent effect of BisQ or AzoCholine on  $\alpha 7$ /GlyR chimera expressed in HEK293T cells. Light was switched between 360 and 440 nm. (a) BisQ (50  $\mu$ M) did not induce a photocurrent, whereas (b) AzoCholine (50  $\mu$ M) triggered large light-dependent inward currents. (c) Puff application of ACh (50  $\mu$ M) evoked an inward current. (d) Photocurrents normalized to ACh puff application, represented as relative currents ( $n = 5$ ). (e) Reversibility of AzoCholine switching on  $\alpha 7$ /GlyR chimera. Traces a–c were recorded from the same cell; bars represent mean; error bars represent SEM.

the switching wavelengths (360 and 440 nm) over many cycles (Figure 3e). In addition, the on and off kinetics of receptor activation and inactivation with AzoCholine were faster compared to those for ACh ( $\tau_{\text{on AzoCholine}} = 3.207 \pm 0.421$  s and  $\tau_{\text{off AzoCholine}} = 1.352 \pm 0.202$  s;  $\tau_{\text{on ACh}} = 4.179 \pm 0.990$  s and  $\tau_{\text{off ACh}} = 2.089 \pm 0.509$  s;  $n = 4$ ). Using current-clamp measurements, we observed a quick and pronounced change of the membrane potential when alternating the illumination between 360 and 440 nm (Figure S5a). As with all PCLs, the effective agonist concentration can be adjusted using different wavelengths of light, allowing for discrete levels of activation of the receptor (Figure S5b,c).

**BisQ, but not AzoCholine, Is a Photoswitchable Agonist for the Muscle nAChR.** To investigate muscle-type receptors, the human  $\alpha 1$ ,  $\beta 1$ ,  $\delta$ , and  $\epsilon$  nAChR subunits were expressed in HEK293T cells. In accordance with Erlanger's results, BisQ proved to be a photoswitchable agonist at the muscle receptor (Figure 4a,e). Action spectra were

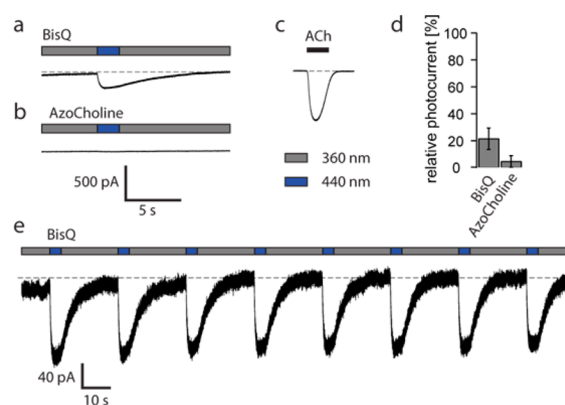


**Figure 4.** Light-dependent effect of BisQ or AzoCholine on neuromuscular nAChR expressed in HEK293T cells. (a) BisQ (50  $\mu\text{M}$ ) evoked light-dependent currents when light was switched between 360 and 440 nm. (b) AzoCholine (50  $\mu\text{M}$ ) did not trigger light-dependent currents. (c) Puff application of ACh (50  $\mu\text{M}$ ) evoked an inward current. (d) Photocurrents normalized to ACh puff application, represented as relative currents ( $n = 5$ ). (e) Reversibility of BisQ switching on neuromuscular nAChR. Traces a–c were recorded from the same cell; bars represent mean; error bars represent SEM.

recorded to determine the best switching wavelengths (Figure S6). While the absorption in the UV/vis measurements would suggest that the best *trans* to *cis* conversion was at 340 nm, due to the optics of the microscope, with reduced transmissibility in the UV-range ( $<350$  nm), the best switching was achieved with 360 and 440 nm light. Washing in a solution of BisQ (50  $\mu\text{M}$ ) irradiated with 360 nm activated the receptor with a transient peak current, which desensitized to a plateau current (Figure S7). This might be due to residual *trans*-BisQ in the solution. When switched to *trans* with 440 nm, BisQ triggered light-dependent currents ( $156.38 \pm 49.13$  pA). Reversibility of currents was achieved over multiple cycles (Figure 4e). When compared to puff-applied ACh at equal concentration, BisQ showed  $21.47 \pm 7.97\%$  activation (Figure 4c,d). However, the kinetics of switching proved to be 2–3 times slower than those observed after ACh puff application ( $\tau_{\text{on ACh}} = 0.106 \pm 0.059$  s and  $\tau_{\text{off ACh}} = 1.515 \pm 0.648$  s;  $\tau_{\text{on BisQ}} = 0.201 \pm 0.025$  s and  $\tau_{\text{off BisQ}} = 4.364 \pm 0.369$  s;  $n = 5$ ).

Washing in a solution of AzoCholine (50  $\mu\text{M}$ ) irradiated with 360 nm activated the receptor with a transient peak current, followed by deactivation. Subsequent irradiation with 440 nm, however, did not change the current amplitude ( $3.64 \pm 13.16$  pA,  $0.77 \pm 1.82\%$  normalized to ACh; Figure 4b,d). Therefore, AzoCholine does not function as a photoswitchable agonist for neuromuscular nAChRs.

**AzoCholine Activates  $\alpha 7$  nAChRs in Rat Primary Afferent DRG Neurons.** Cell bodies of primary afferent neurons conveying sensory information from the periphery toward the spinal cord reside in distinct aggregations termed dorsal root ganglia (DRG). With respect to their responsiveness to mechanical and chemical stimuli, including cholinergic agonists, they represent a heterogeneous population. In rat DRG, the proportion of  $\alpha 7$  nAChR-expressing neurons is higher than that in mice, and the vast majority of them have nociceptor properties in that it responds to potential noxious stimuli.<sup>24–26</sup> Activation of  $\alpha 7$  nAChR results in an increase of intracellular calcium concentration ( $[\text{Ca}^{2+}]_i$ ) in these neurons.<sup>24,25,27</sup> Illumination of isolated and cultured DRG neurons bathed in 250  $\mu\text{M}$  AzoCholine with 460 nm light for 10 s caused a repeatable  $[\text{Ca}^{2+}]_i$  increase in 77 out of 180 cases, which was higher than that evoked by depolarizing the cells with 30 mM KCl (Figure 5) and absent in AzoCholine-free

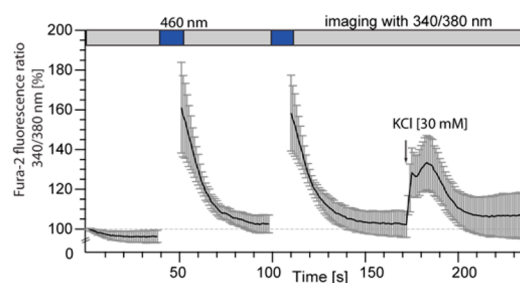


**Figure 5.** Light-dependent effect of AzoCholine on rat sensory neurons isolated from dorsal root ganglia. Illumination with 460 nm light in the presence of AzoCholine (250  $\mu\text{M}$ ) leads to an increase in  $[\text{Ca}^{2+}]_i$ . Depolarization by application of 30 mM KCl with subsequent increase in  $[\text{Ca}^{2+}]_i$  served as control for viability of sensory neurons. The graph depicts mean and standard deviation of data recorded from 77 responsive cells; an additional 103 cells included in the experiment were unresponsive to AzoCholine.

media ( $n = 27$  cells, pooled from four experiments; Figure S8a). Measurement of  $[\text{Ca}^{2+}]_i$  with the calcium-sensitive dye Fura-2 is based upon recording of fluorescence intensity at wavelengths longer than 440 nm. Hence, photoactivation of AzoCholine with 460 nm light interfered with  $[\text{Ca}^{2+}]_i$  recording for the period of stimulation so that immediate poststimulation values, but not the peak height, of  $[\text{Ca}^{2+}]_i$  increase could be determined. This PCL-induced increase in  $[\text{Ca}^{2+}]_i$  was indeed due to nAChR activation since it was not observed in the presence of the  $\alpha 7$  nAChR antagonist, MG624 (50  $\mu\text{M}$ ;  $n = 21$  cells, pooled from four experiments; Figure S8b). In mammals, MG624 also exhibits antagonistic properties to nAChR subunits other than  $\alpha 7$ ,<sup>28</sup> and such nAChRs are also expressed in rat DRG neurons.<sup>24,25</sup> Thus, this pharmacological profile alone does not allow us to qualify the response as being  $\alpha 7$  nAChR-specific. However, the relative number of responsive neurons provides additional supportive evidence for selective stimulation of  $\alpha 7$  nAChRs by photoactivated AzoCholine. We observed  $[\text{Ca}^{2+}]_i$  rises in 43% (77/180) of neurons investigated,

which nicely falls into the range of 35–47% (depending on postnatal age) of rat DRG neurons expressing  $\alpha 7$  nAChRs either alone or in combination with other nAChR, whereas the total fraction of nAChRs carrying neurons amounts to 69–78%.<sup>25</sup> It should be noted that MG624 (Figure 1b) closely resembles AzoCholine but bears a trimethylammonium head-group instead of a triethylammonium moiety.

**AzoCholine Activates  $\alpha 7$  nAChRs in Mouse Hippocampus.** To investigate the effect of AzoCholine on intact neural networks, we performed extracellular electrophysiological recordings in mouse hippocampal brain slices on a multielectrode array (MEA) (Figure S9a). As expected, illumination of the brain slice did not alter bursting activity (Figure S9b). The same is true when washing in AzoCholine (50  $\mu$ M) in the dark (Figure S9c). However, in the presence of AzoCholine, the neuronal activity could be modulated by toggling between 360 and 460 nm (Figure 6a). In accordance

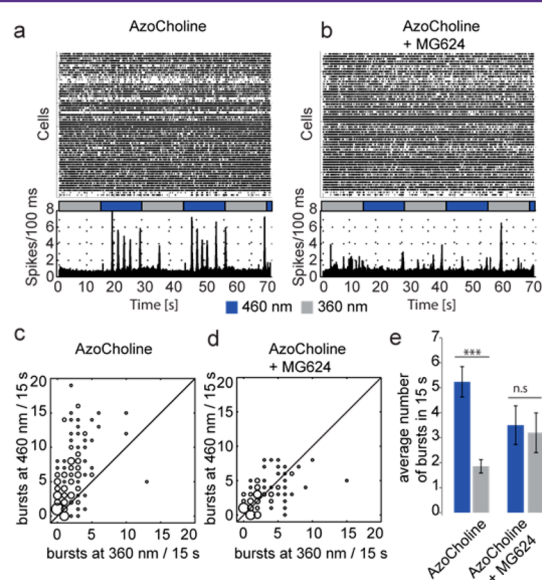


**Figure 6.** Bursting activity in mouse hippocampal brain slices. (a) Raster plot of single-cell spiking activity in the presence of AzoCholine (50  $\mu$ M) with the correlating histograms over all cells. Switching light from 360 nm (gray bar) to 460 nm (blue bar) leads to an increase in bursting activity and vice versa. (b) Raster plot in the presence of AzoCholine (50  $\mu$ M) and MG624 (5  $\mu$ M) with the correlating histogram. Switching of light has no apparent effect on the spiking activity. (c) Quantification of bursting activity of all experiments with AzoCholine ( $n = 6$  experiments with 173 bursting cells) with the dot size related to the number of cells responding. (d) Quantification of bursting activity of all experiments with AzoCholine and MG624 ( $n = 6$  experiments with 121 bursting cells). (e) Summary of all experiments ( $n = 6$ , bars represent mean, error bars represent SEM;  $t$ -test: \*\*\* $p < 0.001$  for AzoCholine only and  $p > 0.05$  with MG624).

with the HEK cell data, blue light increased and violet light decreased bursting activity. Quantified over all experiments, the switching effect is shown in Figure 6c,e (six experiments,  $n = 173$  cells,  $p < 0.001$ ). To confirm that the  $\alpha 7$  nAChR is the target receptor of AzoCholine in hippocampal cells, we coapplied the  $\alpha 7$  nAChR-specific antagonist, MG624 (5  $\mu$ M). Matching the previous results from rat DRG neurons, changes could not be evoked in the presence of the antagonist (Figure 6b); however, basal bursting activity could still be detected (Figure 6d,e; six experiments,  $n = 121$  cells,  $p > 0.05$ ).

**AzoCholine Evokes Light-Dependent Behavior in *Caenorhabditis elegans*.** In liquid medium, the nematode *C. elegans* exhibits a dorso-ventrally alternating c-shaped body posture to achieve swimming locomotion. These thrashing movements can be used to quantify locomotion behavior and motility related phenotypes. Locomotion in the nematode involves neuromuscular as well as neuron–neuron cholinergic synaptic transmission.<sup>29</sup> Furthermore, due to the transparency of the animal, light-based methods like calcium imaging and optogenetics are often used to study neural circuits.<sup>30</sup> As *C. elegans* shows photophobic responses to UV/blue light, mediated by a photosensor, LITE-1,<sup>31</sup> mutants lacking this receptor are often used in optogenetic analyses of behavior.<sup>32</sup> Swimming behavior of *lite-1* animals in physiological buffer (M9) was not affected when switching from UV (350 nm) to blue (470 nm) light illumination (Video S1 and Figure 7).

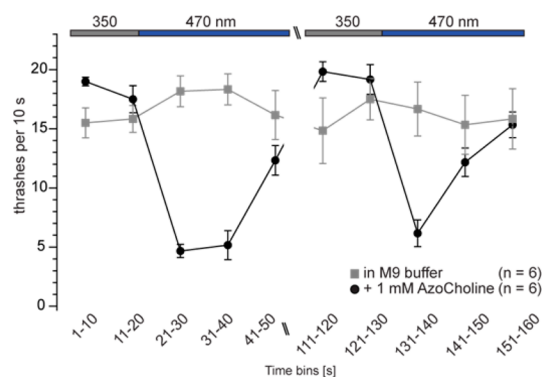


**Figure 7.** Quantification of *C. elegans* swimming cycles. Nematodes swimming in M9 buffer (gray boxes) and in M9 with AzoCholine (1 mM, black circles) ( $n = 6$ ). When switching from UV (350 nm) to blue (470 nm) light (bar), *trans*-AzoCholine induces stopping/freezing behavior in swimming *C. elegans* nematodes.

Notably, when the buffer was supplemented with 1 mM AzoCholine, the nematodes showed a sharp decline in thrashing frequency upon switching from UV to blue light (Video S2). The thrashing frequency recovered during the second half of the light pulse and was fully restored after switching to UV light. This indicates that AzoCholine may have activated nAChRs in the motor nervous system, possibly evoking inhibition, e.g., through GABAergic motoneurons. Interestingly, when tested on wild-type nematodes (strain N2, with normal LITE-1 function) the light-effect of AzoCholine photoswitching did not appear (Video S3 and Figure S10). This unexpected result is intriguing and difficult to rationalize given the complexity of the system. However, we hypothesize that the UV pre-exposure leads to a LITE-1-dependent signal that could put wild-type animals into a state where AzoCholine cannot exert full effects, e.g., because general excitability of the motor system is reduced or AChRs are modified such that they desensitize more readily upon AzoCholine binding. Given the demonstrated specificity of AzoCholine for  $\alpha 7$  nAChRs in mammalian cells, the observed effects in *C. elegans* are likely affected via nAChRs. However, the putative target receptor triggered by AzoCholine in *C. elegans* remains to be validated.

## CONCLUSIONS

In summary, we have re-evaluated the first photochromic ligand for ion channels, BisQ, using the methods of modern channel physiology. As expected, BisQ acts on the neuromuscular

nAChR, but it does not affect neuronal  $\alpha 7$  type nAChRs, at least not in a light-dependent fashion.

Furthermore, we have developed AzoCholine, a PCL that targets  $\alpha 7$  nAChRs, which enables us to control cholinergic systems in various organisms with light. In addition to its photoswitchability, AzoCholine showed faster activation and higher potency than that of the native ligand, ACh. It can be applied in neuronal tissues and works in living animals, as it is able to perturb swimming behavior of *C. elegans* (*lite-1*) in a light-dependent manner.

The main advantage of PCLs when compared to other available tools for light-dependent control of cellular processes is their ease of use. Since no genetic manipulation is required, the compounds can simply be applied like drugs, endowing endogenous receptors with light sensitivity. As such, AzoCholine turns  $\alpha 7$  nAChRs into photoreceptors. By varying the wavelengths, the concentration of the active form of AzoCholine can be adjusted in a graded fashion (photodosing). Thus, it is now feasible to control endogenous nAChRs with high spatiotemporal precision. This will be instrumental for elucidating their roles in the nervous system and may prove to be therapeutically useful.

## METHODS

**Cell Culture.** HEK293T cells were maintained in Dulbecco's modified Eagle's medium (Biochrom, Merk Millipore, Germany) supplemented with 10% fetal calf serum (Biochrom, Merk Millipore, Germany) at 37 °C in a 10% CO<sub>2</sub> atmosphere. Transfections were performed with JetPrime (Polyplus-transfections, France) according to the manufacturer's instructions 24 h before measurements. For muscle nAChR expression, cells were transfected with human  $\alpha 1$ -GFP,  $\beta 1$ ,  $\delta$ , and  $\epsilon$  nAChR subunits in pCDNA3.1 plasmid DNA (each using 125 ng of DNA per coverslip, provided by A. Mourot, Paris). For  $\alpha 7$ /GlyR expression, cells were transfected with  $\alpha 7$ /GlyR DNA in pMT3 (500 ng of DNA per coverslip, provided by T. Grutter, Strasbourg) together with 50 ng per coverslip of yellow fluorescent protein (YFP) plasmid DNA. As controls, nontransfected HEK cells with PCL present and with light switching were used. No photocurrent was detected. Also, transfected HEK cells without the PCL and with light switching gave no photocurrent.

**Tissue Preparation.** Horizontal brain slices preparations from C57BL/6J mice (wild type) were prepared as reported elsewhere.<sup>29</sup> Briefly, mice were decapitated, the brain was removed, and 250  $\mu$ m horizontal slices were prepared using a vibrating microtome (7000smz-2, Campden Instruments, England). Slices were incubated in carbogenated (5% CO<sub>2</sub>, 95% O<sub>2</sub>) sucrose medium (mM: 87 NaCl, 2.5 KCl, 7 MgCl<sub>2</sub>, 0.5 CaCl<sub>2</sub>, 25 Gluc, 1.25 NaH<sub>2</sub>PO<sub>4</sub>, 25 NaHCO<sub>3</sub>, 75 sucrose) for 30 min at 34 °C.

Dorsal root ganglion (DRG) neurons were isolated from male and female Wistar rats (250–300 g body weight) and cultured as described previously.<sup>33</sup> Briefly, DRGs dissected from rat were incubated in an enzyme mixture containing 2 mg/mL collagenase type 1 and 2 mg/mL Dispase II (Sigma-Aldrich, Germany) in calcium and magnesium-free Hanks' balanced salt solution (Life Technologies, Germany) for 15 min at 37 °C in a water bath. Thereafter, DRGs were mechanically dissociated with a glass Pasteur pipette. The process of incubation and mechanical dissociation was repeated two times until the DRGs were completely dissociated. Then, the cells were suspended in L-15 medium (Life Technologies, Germany) containing 10% fetal bovine serum (FBS) and 1% penicillin and streptomycin and centrifuged at 800g for 4 min. This wash and centrifugation was repeated two times. The cell pellet was then resuspended in the same medium, and a small portion (10  $\mu$ L) of the cell suspension was transferred on poly-D-lysine/laminin (Sigma-Aldrich, Germany) coated glass coverslips and incubated at 37 °C for 2 h for the attachment of the neurons to the glass surface. Additional growth medium was added to the wells

containing coverslips, and cells were allowed to stabilize for a further 2 h before calcium measurements were performed.

**Electrophysiology.** Whole-cell patch-clamp recordings were performed with an EPC10 USB patch Clamp amplifier and PatchMaster software (HEKA Elektronik, Germany). Cells were maintained at room temperature and held at  $-60$  mV during the experiments. Micropipettes were generated from GB200-F-8P capillaries (Science Products, Germany) using a vertical puller (PC-10, Narishige, Japan). Pipette resistance varied between 5 and 8 M $\Omega$ . Bath solution contained (in mM) 140 NaCl, 2 Cl, 2 CaCl<sub>2</sub>, 2 MgCl<sub>2</sub>, 10 D-glucose, and 10 HEPES (NaOH to pH 7.4). Pipette solution for muscle nAChR contained (in mM) 140 K-gluconate, 4 NaCl, 12 KCl, 10 HEPES, 4 MgATP, and 0.4 Na<sub>2</sub>-ATP (KOH to pH 7.3). Pipette solution for  $\alpha 7$ /GlyR contained (in mM) 140 CsCl<sub>2</sub>, 10 HEPES 2 Na<sub>2</sub>-ATP, and 10 EGTA (KOH to pH 7.3).

**Multielectrode Array.** Multielectrode array (MEA) of mouse horizontal brain slices was recorded with a Multichannel Systems MEA setup (C57BL/6J mice aged p7 to p13). Slices were placed and oriented with the hippocampus onto the electrodes (Figure S9). To increase basal spiking rate, we increased extracellular potassium to 7.5 mM. Neural bursting activity is defined as more than two recorded action potentials in 2 ms.

**Calcium Measurements.** The intracellular calcium concentration measurements were performed on freshly isolated and DRG neurons (wild-type rats weighing 250–300 g; this corresponds to 9–10 week old animals). All measurements were performed in oxygenated Locke's buffer (pH 7.4) containing (in mM) 14.3 NaHCO<sub>3</sub>, 1.2 NaH<sub>2</sub>PO<sub>4</sub>, 5.6 KCl, 136 NaCl, 1.2 MgCl<sub>2</sub>, 2.2 CaCl<sub>2</sub>, and 10 D-glucose at constant temperature, 34 °C. The cells were loaded with the calcium-sensitive dye, Fura-2 (1  $\mu$ M; Life Technologies, Germany), for 30 min at 37 °C in Locke's buffer and were washed for 10 min in dye-free Locke's buffer solution. Fura-2 is a ratiometric calcium-sensitive dye. It was excited at 340 and 380 nm wavelengths, and its emission peaks at 510 nm. Recordings were done using a fluorescence microscope (Olympus, Hamburg, Germany) connected to a scan CCD camera with fast monochromator (TiLL Photonics, Gräfelfing, Germany). The barrier filter set allows transmission of wavelengths longer than 440 nm. Hence, photoactivation of AzoCholine with 460 nm light interfered with recordings for the period of stimulation so that immediate poststimulation values but not peak height of signal increase could be determined. Each cell was observed separately, and fluorescence intensity at the beginning of the experiment ratio was set to 100%. Light stimulus to activate the photoswitch was applied by a blue light LED.

**Swimming Assay with *Caenorhabditis elegans*.** *C. elegans lite-1* (*ce314*) mutant strain and wild type (N2) were reared using standard methods on nematode growth medium (NGM) and fed *Escherichia coli* strain OP50-1.<sup>34</sup> For the analysis of the behavior of *C. elegans* in liquid, thrashing (swimming) assays of young adult hermaphrodites were carried out in 96-well microtiter plates, containing 100  $\mu$ L of NGM and 100  $\mu$ L of M9 saline solution with or without AzoCholine (1 mM) per well. For the control condition (without AzoCholine), M9 was supplemented with 1% DMSO (carrier solvent for AzoCholine). The animals were incubated in the buffer solution for 15 min under low-intensity UV light. Subsequent UV and blue light illumination of the worms was provided through a 4 $\times$  magnification objective. Assays were recorded with a Powershot G9 camera (Canon, Krefeld, Germany), and swimming cycles (the worm's body bends forth and back per each cycle) were counted for defined time intervals during the UV and blue light illumination. M9 buffer contained (in mM) 20 KH<sub>2</sub>PO<sub>4</sub>, 40 Na<sub>2</sub>HPO<sub>4</sub>, 85 NaCl, and 1 MgSO<sub>4</sub>. Nematode growth medium (NGM) contained 1.7% (w/v) agar-agar, 0.25% (w/v) tryptone/peptone, 0.3% (w/v) NaCl, 0.0005% (w/v) cholesterol (in EtOH), 0.001% (w/v) nystatin, and (in mM) 1 CaCl<sub>2</sub>, 1 MgSO<sub>4</sub>, and 25 K<sub>3</sub>PO<sub>4</sub>.

**Illumination.** For illumination during electrophysiology and UV/vis experiments, a TiLL Photonics Polychrome 5000 monochromator was operated with the HEKA patchmaster software via the patch clamp amplifier or the PolyCon software, respectively. For MEA and DRG experiments, high-power LEDs (460 nm, 9 mW/cm<sup>2</sup>; 365 nm,

1.5 mW/cm<sup>2</sup>) were operated with the HEKA patchmaster software via the patch clamp amplifier. For the nematode swimming assay, a low-intensity UV lamp (366 nm, 16 μW/mm<sup>2</sup>, Benda, Wiesloch, Germany) was used for preillumination during incubation. During the assay, a HBO lamp was used with UV and blue light filters (Zeiss; 325–375 nm, 0.26 mW/mm<sup>2</sup>; 450–490 nm, 0.6 mW/mm<sup>2</sup>).

## ■ ASSOCIATED CONTENT

### ● Supporting Information

Synthesis and characterization of organic compounds and additional photochemical and biological characterization. This material is available free of charge via the Internet at <http://pubs.acs.org>.

## ■ AUTHOR INFORMATION

### Corresponding Author

\*E-mail: [dirk.trauner@lmu.de](mailto:dirk.trauner@lmu.de).

### Author Contributions

D.T., M.P.S., A.G., and A.D. designed the study. J.B., T.U., K.H., D.H.W., and M.S. performed chemical synthesis. M.S., A.D., and K.H. performed UV/vis experiments. A.D. performed the patch-clamp experiments. L.L. and A.D. designed and performed MEA experiments. A.R. and W.K. designed and performed DRG experiments. J.N., A.D., and A.G. designed and performed *C. elegans* experiments. A.D., J.B., K.H., M.S., and D.T. wrote the manuscript through contributions of all authors. All authors have given approval to the final version of the manuscript.

### Funding

D.T. was supported by an Advanced Grant from the European Research Council (268795). A.D., M.S., and L.L. were supported by the International Max Planck Research School for Molecular and Cellular Life Sciences (IMPRS-LS). J.B. was supported by a Ph.D. fellowship from the Studienstiftung des Deutschen Volkes. W.K. was supported by the LOEWE Research Focus Non-neural Cholinergic Systems. J.N. was supported by the Deutsche Forschungsgemeinschaft (DFG) within grant FOR1279 to A.G. and D.T.

### Notes

The authors declare no competing financial interest.

## ■ ACKNOWLEDGMENTS

The authors gratefully acknowledge Dr. D. Barber for helpful discussions, L. de la Osa de la Rosa for technical assistance, and Dr. P. Mayer for crystal structure elucidations. Plasmid containing the α7/GlyR construct was a generous gift from Prof. Dr. T. Grutter. Plasmids for neuromuscular nAChR were generous gifts from Dr. A. Mourot.

## ■ ABBREVIATIONS

nAChR, nicotinic acetylcholine receptor; mAChR, muscarinic acetylcholine receptor; RT, room temperature; GlyR, glycine receptor; HEK293T cells, human embryonic kidney cells type 293T; PCL, photochromic ligand; DRG, dorsal root ganglion; UV, ultraviolet; MEA, multielectrode array

## ■ REFERENCES

(1) Kalamida, D., Poulas, K., Avramopoulou, V., Fostieri, E., Lagoumintzis, G., Lazaridis, K., Sideri, A., Zouridakis, M., and Tzartos, S. J. (2007) Muscle and neuronal nicotinic acetylcholine receptors. Structure, function and pathogenicity. *FEBS J.* 274, 3799–845.

(2) Lemoine, D., Jiang, R., Taly, A., Chataigneau, T., Specht, A., and Grutter, T. (2012) Ligand-gated ion channels: new insights into neurological disorders and ligand recognition. *Chem. Rev.* 112, 6285–318.

(3) Bartels, E., Wassermann, N. H., and Erlanger, B. F. (1971) Photochromic activators of the acetylcholine receptor. *Proc. Natl. Acad. Sci. U.S.A.* 68, 1820–3.

(4) Beith, J., Wassermann, N., Vratisanos, S. M., and Erlanger, B. F. (1970) Photoregulation of biological activity by photochromic reagents, IV. A model for diurnal variation of enzymic activity. *Proc. Natl. Acad. Sci. U.S.A.* 66, 850–854.

(5) Deal, W. J., Erlanger, B. F., and Nachmansohn, D. (1969) Photoregulation of biological activity by photochromic reagents. 3. Photoregulation of bioelectricity by acetylcholine receptor inhibitors. *Proc. Natl. Acad. Sci. U.S.A.* 64, 1230–4.

(6) Lester, H. A., Krouse, M. E., Nass, M. M., Wassermann, N. H., and Erlanger, B. C. (1980) A covalently bound photoisomerizable agonist: comparison with reversibly bound agonists at *Electrophorus electroplaques*. *J. Gen. Physiol.* 75, 207–232.

(7) Nargeot, J., Lester, H. A., Birdsall, N. J., Stockton, J., Wassermann, N. H., and Erlanger, B. C. (1982) A photoisomerizable muscarinic antagonist. Studies of binding and of conductance relaxations in frog heart. *J. Gen. Physiol.* 79, 657–678.

(8) Gurney, A. M., and Lester, H. A. (1987) Light-flash physiology with synthetic photosensitive compounds. *Physiol. Rev.* 67, 583–617.

(9) Fehrentz, T., Schonberger, M., and Trauner, D. (2011) Optochemical genetics. *Angew. Chem., Int. Ed.* 50, 12156–82.

(10) Velema, W. A., Szymanski, W., and Feringa, B. L. (2014) Photopharmacology: beyond proof of principle. *J. Am. Chem. Soc.* 136, 2178–91.

(11) Tochitsky, I., Banghart, M. R., Mourot, A., Yao, J. Z., Gaub, B., Kramer, R. H., and Trauner, D. (2012) Optochemical control of genetically engineered neuronal nicotinic acetylcholine receptors. *Nat. Chem.* 4, 105–11.

(12) Banghart, M., Borges, K., Isacoff, E., Trauner, D., and Kramer, R. H. (2004) Light-activated ion channels for remote control of neuronal firing. *Nat. Neurosci.* 7, 1381–6.

(13) Stawski, P., Sumser, M., and Trauner, D. (2012) A photochromic agonist of AMPA receptors. *Angew. Chem., Int. Ed.* 51, 5748–51.

(14) Stein, M., Middendorp, S. J., Carta, V., Pejo, E., Raines, D. E., Forman, S. A., Sigel, E., and Trauner, D. (2012) Azo-propofols: photochromic potentiators of GABA(A) receptors. *Angew. Chem., Int. Ed.* 51, 10500–4.

(15) Wyart, C., Del Bene, F., Warp, E., Scott, E. K., Trauner, D., Baier, H., and Isacoff, E. Y. (2009) Optogenetic dissection of a behavioural module in the vertebrate spinal cord. *Nature* 461, 407–10.

(16) Mourot, A., Fehrentz, T., Le Feuvre, Y., Smith, C. M., Herold, C., Dalkara, D., Nagy, F., Trauner, D., and Kramer, R. H. (2012) Rapid optical control of nociception with an ion-channel photoswitch. *Nat. Methods* 9, 396–402.

(17) Lemoine, D., Habermacher, C., Martz, A., Mery, P. F., Bouquier, N., Diverchy, F., Taly, A., Rassendren, F., Specht, A., and Grutter, T. (2013) Optical control of an ion channel gate. *Proc. Natl. Acad. Sci. U.S.A.* 110, 20813–8.

(18) Levitz, J., Pantoja, C., Gaub, B., Janovjak, H., Reiner, A., Hoagland, A., Schoppik, D., Kane, B., Stawski, P., Schier, A. F., Trauner, D., and Isacoff, E. Y. (2013) Optical control of metabotropic glutamate receptors. *Nat. Neurosci.* 16, 507–16.

(19) Schonberger, M., and Trauner, D. (2014) A photochromic agonist for mu-opioid receptors. *Angew. Chem., Int. Ed.* 53, 3264–7.

(20) Broichhagen, J., Jurastow, I., Iwan, K., Kummer, W., and Trauner, D. (2014) Optical control of acetylcholinesterase with a tacrine switch. *Angew. Chem., Int. Ed.* 53, 7657–60.

(21) Unwin, N. (2005) Refined structure of the nicotinic acetylcholine receptor at 4 Å resolution. *J. Mol. Biol.* 346, 967–89.

(22) Grutter, T., de Carvalho, L. P., Dufresne, V., Taly, A., Edelstein, S. J., and Changeux, J. P. (2005) Molecular tuning of fast gating in

pentameric ligand-gated ion channels. *Proc. Natl. Acad. Sci. U.S.A.* 102, 18207–12.

(23) Craig, P. J., Bose, S., Zwart, R., Beattie, R. E., Folly, E. A., Johnson, L. R., Bell, E., Evans, N. M., Benedetti, G., Pearson, K. H., McPhie, G. I., Volsen, S. G., Millar, N. S., Sher, E., and Broad, L. M. (2004) Stable expression and characterisation of a human alpha 7 nicotinic subunit chimera: a tool for functional high-throughput screening. *Eur. J. Pharmacol.* 502, 31–40.

(24) Haberberger, R. V., Bernardini, N., Kress, M., Hartmann, P., Lips, K. S., and Kummer, W. (2004) Nicotinic acetylcholine receptor subtypes in nociceptive dorsal root ganglion neurons of the adult rat. *Auton. Neurosci.* 113, 32–42.

(25) Smith, N. J., Hone, A. J., Memon, T., Bossi, S., Smith, T. E., McIntosh, J. M., Olivera, B. M., and Teichert, R. W. (2013) Comparative functional expression of nAChR subtypes in rodent DRG neurons. *Front. Cell. Neurosci.* 7, 225.

(26) Shelukhina, I., Paddenberger, R., Kummer, W., and Tsetlin, V. (2014) Functional expression and axonal transport of alpha7 nAChRs by peptidergic nociceptors of rat dorsal root ganglion. *Brain Struct. Funct.*, DOI: 10.1007/s00429-014-0762-4.

(27) Fucile, S., Supapane, A., and Eusebi, F. (2005) Ca<sup>2+</sup> permeability of nicotinic acetylcholine receptors from rat dorsal root ganglion neurones. *J. Physiol.* 565, 219–28.

(28) Gotti, C., Carbonnelle, E., Moretti, M., Zwart, R., and Clementi, F. (2000) Drugs selective for nicotinic receptor subtypes: a real possibility or a dream? *Behav. Brain Res.* 113, 183–92.

(29) Schoenberger, M., Damijonaitis, A., Zhang, Z., Nagel, D., and Trauner, D. (2014) Development of a new photochromic ion channel blocker via azologization of fomocaine. *ACS Chem. Neurosci.* 5, 514–518.

(30) de Bono, M., Schafer, W. R., and Gottschalk, A. (2013) Optogenetic actuation, inhibition, modulation and readout for neuronal networks generating behavior in the nematode *Caenorhabditis elegans*, in *Optogenetics* (Hegemann, P., and Sigrist, S., Eds.) pp 61–78, De Gruyter, Berlin.

(31) Edwards, S. L., Charlie, N. K., Milfort, M. C., Brown, B. S., Gravlin, C. N., Knecht, J. E., and Miller, K. G. (2008) A novel molecular solution for ultraviolet light detection in *Caenorhabditis elegans*. *PLoS Biol.* 6, e198.

(32) Husson, S. J., Costa, W. S., Wabnig, S., Stirman, J. N., Watson, J. D., Spencer, W. C., Akerboom, J., Looger, L. L., Treinin, M., Miller, D. M., III, Lu, H., and Gottschalk, A. (2012) Optogenetic analysis of a nociceptor neuron and network reveals ion channels acting downstream of primary sensors. *Curr. Biol.* 22, 743–52.

(33) Nassenstein, C., Taylor-Clark, T. E., Myers, A. C., Ru, F., Nandigama, R., Bettner, W., and Udem, B. J. (2010) Phenotypic distinctions between neural crest and placodal derived vagal C-fibres in mouse lungs. *J. Physiol.* 588, 4769–83.

(34) Brenner, S. (1974) The genetics of *Caenorhabditis elegans*. *Genetics* 77, 71–94.